Eur Radiol
DOI 10.1007/s00330-015-3985-8

MAGNETIC RESONANCE

Accelerated magnetic resonance diffusion tensor imaging of the median nerve using simultaneous multi-slice echo planar imaging with blipped CAIPIRINHA

Lukas Filli[1] · Marco Piccirelli[2] · David Kenkel[1] · Andreas Boss[1] · Andrei Manoliu[1] · Gustav Andreisek[1] · Himanshu Bhat[3] · Val M. Runge[1] · Roman Guggenberger[1]

Received: 28 November 2014 / Revised: 8 August 2015 / Accepted: 31 August 2015

Abstract
Purpose To investigate the feasibility of MR diffusion tensor imaging (DTI) of the median nerve using simultaneous multi-slice echo planar imaging (EPI) with blipped CAIPIRINHA.
Materials and methods After federal ethics board approval, MR imaging of the median nerves of eight healthy volunteers (mean age, 29.4 years; range, 25–32) was performed at 3 T using a 16-channel hand/wrist coil. An EPI sequence (b-value, 1,000 s/mm^2; 20 gradient directions) was acquired without acceleration as well as with twofold and threefold slice acceleration. Fractional anisotropy (FA), mean diffusivity (MD) and quality of nerve tractography (number of tracks, average track length, track homogeneity, anatomical accuracy) were compared between the acquisitions using multivariate ANOVA and the Kruskal-Wallis test.
Results Acquisition time was 6:08 min for standard DTI, 3:38 min for twofold and 2:31 min for threefold acceleration. No differences were found regarding FA (standard DTI: 0.620 ±0.058; twofold acceleration: 0.642±0.058; threefold acceleration: 0.644±0.061; $p \geq 0.217$) and MD (standard DTI: 1.076±0.080 mm^2/s; twofold acceleration: 1.016± 0.123 mm^2/s; threefold acceleration: 0.979±0.153 mm^2/s; $p \geq 0.074$). Twofold acceleration yielded similar tractography quality compared to standard DTI ($p > 0.05$). With threefold acceleration, however, average track length and track homogeneity decreased ($p = 0.004$–0.021).
Conclusion Accelerated DTI of the median nerve is feasible. Twofold acceleration yields similar results to standard DTI.
Key Points
- *Standard DTI of the median nerve is limited by its long acquisition time.*
- *Simultaneous multi-slice acquisition is a new technique for accelerated DTI.*
- *Accelerated DTI of the median nerve yields similar results to standard DTI.*

Keywords Diffusion tensor imaging · Diffusion tractography · Simultaneous multi-slice · Echo-planar imaging · Median nerve

Abbreviations

CAIPIRINHA	Controlled aliasing in parallel imaging results in higher acceleration
DRUJ	Distal radio-ulnar joint
DTI	Diffusion tensor imaging
EPI	Echo planar imaging
FA	Fractional anisotropy
FDi	Fibre density index
ICC	Intra-class correlation coefficient
MD	Mean diffusivity
ROI	Region of interest
SMS	Simultaneous multi-slice acquisition
SNR	Signal-to-noise ratio
TE	Echo time
TR	Repetition time

✉ Lukas Filli
lukas.filli@usz.ch

[1] Institute of Diagnostic and Interventional Radiology, University Hospital of Zurich, University of Zurich, Raemistrasse 100, CH-8091 Zurich, Switzerland

[2] Department of Neuroradiology, University Hospital of Zurich, Zurich, Switzerland

[3] Siemens Medical Solutions USA Inc, Charlestown, MA, USA

Published online: 15 September 2015

Introduction

Magnetic resonance (MR) diffusion tensor imaging (DTI) allows characterization of tissue microstructure by measuring the diffusion of water molecules along at least six different gradient directions, which is usually performed with echo-planar imaging (EPI) [1]. In highly organized tissues, such as peripheral nerves with axon bundles and myelin sheaths, diffusion is anisotropic and predominantly occurs parallel to the course of the fibres. This anisotropy is based on the restriction of diffusion by cellular barriers [2, 3]. With DTI, the three orthogonal main axes of diffusion (eigenvectors) and their respective intensities (eigenvalues), which both characterize respective tensor geometries, can be calculated voxel-wise. Furthermore, the fractional anisotropy (FA) and the mean diffusivity (MD, equal to the apparent diffusion coefficient) can be obtained from the three eigenvalues to further describe the diffusion behaviour [1]. Tractography algorithms allow visualization of the orientation and course of fibres [4, 5] by connecting voxels with similar diffusion properties according to predefined criteria.

In the past years, the potential of MRI for peripheral nerves, including DTI applications, has been elucidated in numerous studies [6–9]. In particular, due to its size and rather superficial location, the median nerve has been extensively investigated and several works have shown the usefulness of DTI in the assessment of diffusion changes with ageing or in pathological conditions, e.g. carpal tunnel syndrome [10–20].

A major challenge in DTI of peripheral nerves is to avoid artefacts and dephasing arising from patient motion and blood pulsation during the examination. Firm fixation of extremities can be troublesome, especially in DTI of the median nerve where patients are usually examined in the uncomfortable 'superman position' with the arm outstretched over head. Therefore, in order to minimize artefacts and to maximize patient comfort, DTI sequences should be as short as possible while maintaining the image quality and signal-to-noise ratio (SNR) sufficient for quantitative measurements and tractography.

Conventional techniques for accelerated imaging, such as parallel imaging [21] or partial Fourier sampling [22], improve the SNR but cannot significantly reduce the acquisition time in single-shot EPI. By contrast, simultaneous multi-slice (SMS) imaging is a promising method, where multiple slices are excited concurrently with a multiband radiofrequency pulse. This technique was first published in 2001 [23], but has only recently gained more extensive interest from the MR community due to the 'Controlled aliasing in parallel imaging results in higher acceleration' (CAIPIRINHA) technique [24] and its implementation to EPI with markedly reduced g-factor penalty (blipped CAIPIRINHA) [25–27].

The aim of the present study was to investigate the feasibility of accelerated DTI of the median nerve using SMS with blipped CAIPIRINHA. The hypothesis was that, compared with standard DTI, this technique would significantly reduce the acquisition time at a comparable functional DTI metrics and image quality.

Materials and methods

Study population

This study was approved by the federal ethics board. Eight healthy volunteers (six males, two females; mean age, 29.4 years; age range, 25–32 years) underwent MRI of their dominant wrist (six right side, two left side). None of them reported previous local surgery or recurring paraesthesia in the respective lower and upper extremity suggestive of peripheral neuropathy. Written informed consent was obtained from all subjects.

Imaging protocol

Imaging was performed on a 3 T scanner (MAGNETOM Skyra, Siemens Healthcare, Erlangen, Germany) with a maximum amplitude of 45 mT/m and a slew rate of 200 T/m/s. All subjects lay in a prone position with the arm extended over the head and aligned to the z-axis of the magnetic field ('superman position') [12, 16]. The wrist was placed in a dedicated 16-channel hand/wrist coil (Siemens Healthcare) positioned in the scanner's isocentre.

All sequences were planned such that they covered the entire carpal tunnel in the transversal orientation. Initially, a T1-weighted SPACE (Sampling Perfection with Application of optimized Contrasts using different flip angle Evolution) sequence for anatomical correlation and exclusion of gross structural abnormalities was acquired (TR, 500 ms; TE, 11 ms; turbo factor, 42; number of slices, 192; slice thickness, 0.8 mm; in-plane resolution, 0.5×0.5 mm^2). Next, DTI was performed based on single-shot EPI with SMS acceleration and blipped CAIPIRINHA using a dedicated software package for research purposes (Siemens Healthcare, Erlangen, Germany). Three different DTI sequences were applied at a b-value of 1,000 s/mm^2 [12] with 20 gradient encoding diffusion directions and a respective slice acceleration factor of 1 (no acceleration, i.e. conventional reference scan comparable to a traditional, 'simple' single-shot EPI sequence), 2 (two simultaneously excited slices) or 3 (three simultaneously excited slices) (Table 1). Each of these three sequences was performed twice for SNR measurements as well as repeatability analysis (see below).

Table 1 Image parameters of the diffusion tensor imaging (DTI) sequences with different slice acceleration factors

	Standard DTI	2× slice acceleration	3× slice acceleration
b-factor (s/mm^2)	1,000	1,000	1,000
Gradient directions	20	20	20
Signal averages (b=0; b=1000)	5; 3	5; 3	5; 3
TR (ms)	5,200	3,000	2,000
TE (ms)	74	74	74
Number of slices	42	42	45 (42 not applicable)
Slice thickness; slice gap (mm)	3; 0	3; 0	3; 0
In-plane resolution (mm^2)	1.4×1.4	1.4×1.4	1.4×1.4
Field of view (mm^2)	140×140	140×140	140×140
Partial Fourier	5/8	5/8	5/8
GRAPPA	2	2	2
Bandwidth (Hz/Px)	1,034	1,034	1,034
Duration (min)	6:08	3:38	2:31

The shim volume was automatically placed and kept constant for all DTI sequences to minimize the influence of b0 heterogeneities.

Post-processing and measurements

Colour-coded FA maps as well as greyscale FA and MD maps were automatically generated by the scanner (Fig. 1). For FA and MD measurements, two independent readers (LF and DK) placed regions of interest (ROIs) on the respective maps in the median nerve at the level of the distal radioulnar joint (DRUJ), the pisiform bone and the hamate bone [13, 15]. The corresponding T1 images were consulted to clearly identify these levels and to align the ROIs to the respective anatomy. Potential partial-volume effects were avoided by defining the ROIs slightly smaller than the cross-sectional area of the nerve [11].

Tractography

Tractography was performed on a commercially available workstation (software 'Neuro 3D', syngo Leonardo, Siemens Healthcare, Erlangen, Germany) by two readers (LF and DK). One seed ROI, which served as starting point for the automatic fibre tracking, was placed at the level of the pisiform bone. In contrast to the aforementioned ROIs for FA/MD measurements, this ROI was drawn exactly along the borders of the nerve to ensure the inclusion of all nerve fibres [13]. Based on the findings of a previous study on optimal fibre tracking of the median nerve at 3 Tesla [12], the FA threshold value and the angulation threshold were set to 0.2 and 10°, respectively.

The tractography performance depending on the slice acceleration factor chosen was assessed in terms of (1) number of tracks, (2) average track length and (3) fibre density index (FDi, i.e. the number of tracts divided by the area of the seed

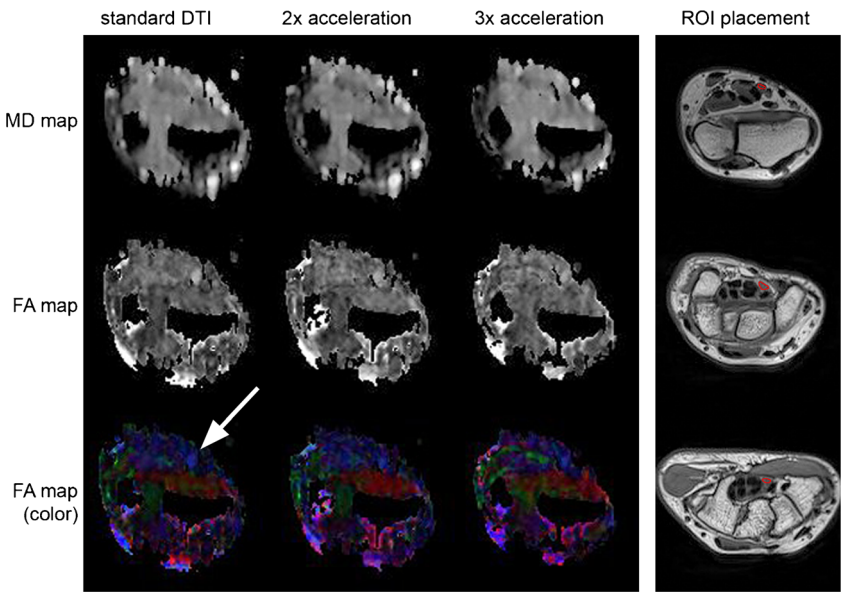

Fig. 1 **Left**: Exemplary mean diffusivity (MD) and fractional anisotropy (FA) maps at the level of the distal radio-ulnar joint, acquired with different slice acceleration factors. The median nerve can be well depicted on the FA maps (arrow), as it runs mainly parallel to the z-axis of the scanner (blue-coded). **Right**: Illustration of region of interest (ROI) placement on T1-weighted images at the level of the distal radio-ulnar joint (top), the pisiform bone (middle) and the hamate bone (bottom)

ROI) [28]. Furthermore, a qualitative 4-point-scale assessment was performed with regard to the track homogeneity (1 = poor, 2 = fair, 3 = good, 4 = excellent) and the anatomical accuracy (i.e. the correspondence of the track to the anatomical fibre course: 1 = poor, 2 = fair, 3 = good, 4 = excellent).

Signal-to-noise ratio (SNR) calculation

All DTI sequences were acquired twice with identical parameters. After subtraction of the images at b=0, respective voxel-by-voxel difference images between the identical sequences could be generated [17, 29]. On these difference images, the standard deviation of the signal intensity ('noise') was measured. The SNR of the median nerve at the level of the pisiform bone was then calculated for the different sequences as follows:

$$SNR = \frac{SI}{noise} \times \sqrt{2} \quad (1)$$

Furthermore, the SNR of each sequence was divided by the respective acquisition time in order to determine the SNR per minute.

Statistical analysis

All statistical analyses were performed with SPSS (v20, IBM Corp., Somers, NY, USA). To assess the inter-reader agreement of FA and MD measurements by both readers, respective intra-class correlation coefficients (ICCs) were calculated. An ICC ≤0.20 indicated slight agreement, 0.21–0.40 fair agreement, 0.41–0.60 moderate agreement, 0.61–0.80 substantial agreement, 0.81–0.99 almost perfect agreement and 1.00 perfect agreement [30]. The inter-observer reliability of track homogeneity and anatomical accuracy scores was quantified by calculating Cohen's kappa.

For further statistical comparisons, FA and MD measurements were averaged between both readers. FA, MD, number of tracks, average track length and FDi were compared between the different sequences by using a multivariate ANOVA with post-hoc Bonferroni tests. Track homogeneity and anatomical accuracy scores were compared using the Kruskal-Wallis test. For all tests, a p-value of <0.05 was considered to indicate statistically significant differences. The correlation between SNR and number of tracks as well as between SNR and average track length was assessed by calculating respective Spearman's correlation coefficients.

Since every DTI sequence was acquired twice, the test-retest reliability of overall FA and MD values between both scans could be analysed by calculating ICCs. For this purpose, one reader (LF) also performed measurements on the second set of images. The dependence of the test-retest reliability from the applied slice acceleration factor was then assessed.

In order to quantify the variability of overall FA and MD values among the individual volunteers, respective coefficients of variation (i.e. the standard deviation divided by the mean) were calculated for all DTI sequences. Again, the dependence of the variation from the slice acceleration factor was determined.

Results

Image acquisition

All images were successfully acquired without the presence of significant motion artefacts in any of the sequences (for exemplary FA and MD maps see Fig. 1). Acquisition time was 6:08 min for standard DTI, 3:38 min for twofold acceleration and 2:31 min for threefold acceleration. The total imaging duration was 28:56 min.

Quantitative measurements

Mean ROI sizes for FA and MD measurements were 7±1 mm^2 (reader 1: 8±1 mm^2; reader 2: 7±1 mm^2). ICC values ranged from 0.801 to 0.871 for FA measurements and from 0.886 to 0.931 for MD measurements, indicating almost perfect inter-reader agreement [30]. Regarding the qualitative ratings, Cohen's kappa was 0.734 for the track homogeneity score and 0.647 for the anatomical accuracy score, indicating fair to good agreement. No significant differences in FA and MD values were found between the sequences with different slice acceleration factors (FA: $p \geq 0.217$; MD: $p \geq 0.074$) (Table 2).

The test-retest reliability of FA and MD measurements was almost perfect regardless of the slice acceleration factor applied. The coefficients of variation of FA and MD values were relatively low in all sequences (Fig. 2).

Tractography

Tractography was successful in all subjects (see example provided in Fig. 3). The number of tracks and the average track length both decreased with increasing slice acceleration, likely due to the lower SNR. Given the high standard deviation, the differences were not statistically significant regarding the number of tracks. However, the average track length decreased significantly (standard DTI vs. threefold slice acceleration: $p=0.018$; twofold vs. threefold slice acceleration: $p=0.010$). Track homogeneity and anatomical accuracy were rated fair to good at standard DTI and twofold slice acceleration, but only poor to fair at threefold slice acceleration (Table 3). There was only a weak positive correlation between SNR and number of tracks (Pearson's correlation coefficient, 0.249) as well as between SNR and average track length (Pearson's correlation coefficient, 0.215).

Table 2 Mean values±standard deviations of fractional anisotropy (FA) and mean diffusivity (MD) in sequences with different slice acceleration measured by two independent readers at the level of the distal radio-ulnar joint (DRUJ), the pisiform bone and the hamate bone

	Standard DTI		2× slice acceleration		3× slice acceleration	
	FA	MD (10^{-3} mm^2/s)	FA	MD (10^{-3} mm^2/s)	FA	MD (10^{-3} mm^2/s)
Reader 1						
Total	0.619±0.051	1.083±0.087	0.648±0.054	1.010±0.125	0.642±0.060	0.974±0.160
DRUJ	0.643±0.025	1.071±0.069	0.619±0.037	1.040±0.187	0.631±0.031	0.998±0.193
Pisiform bone	0.633±0.053	1.099±0.121	0.693±0.051	0.977±0.047	0.666±0.075	0.931±0.190
Hamate bone	0.581±0.052	1.081±0.085	0.631±0.043	1.014±0.115	0.629±0.075	0.993±0.136
Reader 2						
Total	0.621±0.065	1.068±0.074	0.637±0.063	1.021±0.123	0.646±0.063	0.985±0.149
DRUJ	0.620±0.036	1.055±0.055	0.617±0.063	1.038±0.201	0.659±0.046	0.995±0.174
Pisiform bone	0.660±0.052	1.111±0.104	0.697±0.048	1.024±0.051	0.661±0.058	0.967±0.174
Hamate bone	0.583±0.084	1.040±0.055	0.596±0.026	1.001±0.097	0.619±0.062	0.992±0.107
Mean of both readers						
Total	0.620±0.058	1.076±0.080	0.642±0.058	1.016±0.123	0.644±0.061	0.979±0.153
DRUJ	0.631±0.038	1.063±0.065	0.618±0.054	1.039±0.179	0.645±0.058	0.996±0.173
Pisiform bone	0.646±0.054	1.105±0.101	0.695±0.044	1.000±0.053	0.664±0.071	0.949±0.174
Hamate bone	0.582±0.061	1.060±0.068	0.614±0.037	1.007±0.108	0.624±0.050	0.993±0.108
Intra-class correlation coefficient ICC (95 % confidence interval)						
Total	0.801 (0.517–0.919)	0.886 (0.718–0.954)	0.876 (0.700–0.949)	0.931 (0.832–0.972)	0.871 (0.682–0.948)	0.929 (0.827–0.971)

SNR measurements

The measured SNR values at different slice acceleration factors were 19.60±8.98 (standard DTI), 16.32±6.74 (twofold acceleration) and 11.33±3.85 (threefold acceleration), respectively. Consequently, the corresponding SNRs per minute were 3.19±1.46 (standard DTI), 4.49±1.86 (twofold acceleration) and 4.51±1.53 (threefold acceleration).

Discussion

In the present study, the feasibility of accelerated DTI of the median nerve using SMS imaging with blipped CAIPIRINHA was demonstrated and compared to standard DTI.

DTI parameters measured in the standard scan (FA: 0.620±0.058; MD: 1.076±0.080×10^{-3} mm^2/s) were in close agreement with the literature [10, 13, 16, 18] and not significantly influenced by slice acceleration. In agreement with a previous work [13], FA values were lower at the level of the hamate bone than at the level of the DRUJ. The measurements showed almost perfect inter-observer agreement, relatively low variability and good test-retest reliability. There was a trend towards higher FA values with increasing slice acceleration (though not statistically significant), which is a well-recognized though not fully understood phenomenon [31, 32].

With slice acceleration, the measured MD values fell below the reported optimal cut-off value of 1.054×10^{-3} mm^2/s for the diagnosis of carpal tunnel syndrome [13]. However, significant overlaps of diffusion properties of the median nerve among different ages as well as healthy versus pathological conditions were also reported. Nevertheless, the high repeatability and low variability of our measurements indicate a robust technique with potentially high discriminatory

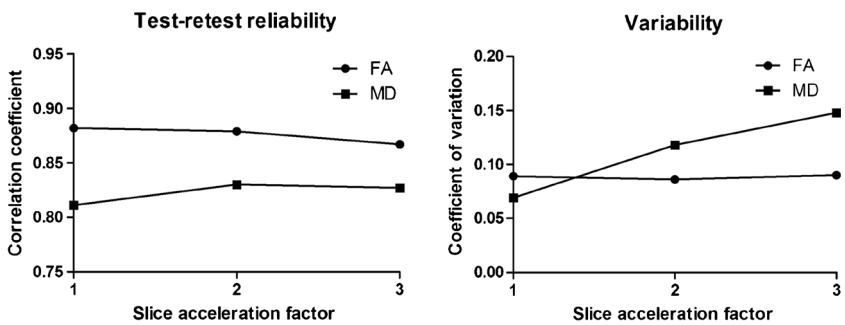

Fig. 2 Dependence of test-retest reliability (ICC) and variability (coefficient of variation) of fractional anisotropy (FA) and mean diffusivity (MD) values from the slice acceleration factor. The slice acceleration factor 1 corresponds to the standard diffusion tensor imaging (DTI) sequence

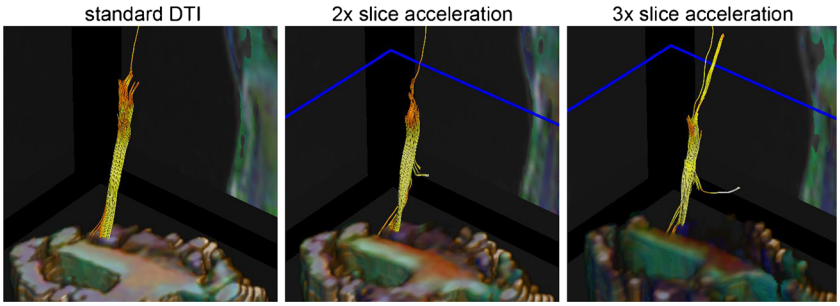

Fig. 3 Exemplary tractography of the median nerve in a 28-year-old male volunteer based on data acquired with standard diffusion tensor imaging (DTI), twofold and threefold slice acceleration. The respective seed regions of interest (ROIs) were drawn at the level of the pisiform bone. Anatomical reference slices are not shown so that the gradually decreasing signal intensity of the DTI data and quality of tractography with increasing slice acceleration can be recognized

performance. Further studies may clarify whether new normative and cut-off values are needed for slice-accelerated sequences. If it remains unclear why DTI parameters are affected by slice acceleration, new normative values may also be necessary for other body regions and pathologies to maintain the level of diagnostic accuracy.

Tractography is a powerful tool for illustrating the fibre course of the median nerve. A previous work found tractography a useful and reproducible tool for analysing the nerve microstructure in patients with carpal tunnel syndrome [17]. In carpal tunnel syndrome, chronic pressure leads to an increase of endoneurial and perineurial connective tissue as well as intrafascicular oedema due to local venous compression. In this case, FA values are decreased because of impaired diffusion of water molecules along the main nerve fibre direction. Thus, the success of tractography is considered an indirect marker for the amount of microstructural alteration.

In our study, tractography in the standard DTI scan delivered similar parameters compared with the literature [12]. Its performance regarding fibre course visualization was similar to twofold slice acceleration but significantly impaired with threefold acceleration, as there was a decrease in the number of tracks, the average track length, track homogeneity and anatomical accuracy. The most likely explanation is that the lower SNR limited automatic fibre tracking because of less

Table 3 Characteristics of tractography based on data of the sequences with different slice acceleration factors (data are presented as mean±standard deviation)

	Standard DTI	2× slice acceleration	3× slice acceleration	Sequences with significant differences
Reader 1				
Number of tracks	835±117	772±255	584±222	–
Average track length (mm)	46.2±4.3	47.2±3.9	35.0±8.0	Standard DTI/3× (p=0.012), 2×/3× (p=0.006)
FDi	16.6±2.1	16.6±1.8	15.6±4.0	–
Track homogeneity	3.2±0.4	2.7±0.5	1.7±0.8	Standard DTI/3× (p=0.007), 2×/3× (p=0.041)
Anatomical accuracy	2.7±0.8	2.2±0.4	1.8±0.4	Standard DTI/3× (p=0.045)
Reader 2				
Number of tracks	796±122	735±253	596±227	–
Average track length (mm)	44.4±4.2	45.3±3.7	34.7±8.1	Standard DTI/3× (p=0.028)
FDi	16.4±2.4	16.4±2.1	18.8±4.4	–
Track homogeneity	3.2±0.8	2.8±0.4	1.7±0.8	–
Anatomical accuracy	2.8±0.8	2.5±0.6	1.8±0.4	Standard DTI/3× (p=0.015)
Mean of both readers				
Number of tracks	816±116	753±252	590±225	–
Average track length (mm)	45.3±4.2	46.3±3.8	34.8±8.0	Standard DTI/3× (p=0.018), 2×/3× (p=0.010)
FDi	16.5±2.3	16.5±1.9	16.4±4.4	–
Track homogeneity	3.2±0.5	2.8±0.4	1.9±0.7	Standard DTI/3× (p=0.004)
Anatomical accuracy	2.8±0.8	2.3±0.4	1.8±0.4	Standard DTI/3× (p=0.021)

The first three parameters were compared by using multivariate ANOVA, the others (qualitative scoring) by using the Kruskal-Wallis test. *FDi* fibre density index

accurate voxel-wise tensor calculation. Nevertheless, as shown above, focal FA and MD measurements were not impaired by slice acceleration.

The SNR of the median nerve on the b0 image of the standard DTI sequence was in the range of the literature [17]. Unlike previous acceleration techniques [24, 33], blipped-CAIPI does not suffer from a relevant g-factor penalty; in the brain, it was shown that the g-factor penalty was only 1 % with threefold slice acceleration at 3 T [25, 34] and thus negligible. The SNR only decreases due to two other effects: (1) the lower TR leads to saturation effects; (2) the decreasing distance between the excited slices hampers their separation (depending on the size and position of the coil elements). Nevertheless, the SNR per time unit is expected to increase until TR is lower than 1.25 T1 [25]. Since the median nerve has a T1 relaxation time of 1410±70 ms at 3 T [35], the TR in our study was theoretically still long enough even at threefold slice acceleration (TR, 2,000 ms) to ensure higher SNR per time unit compared to standard DTI. The results are in agreement with this principle, although the SNR per minute was only slightly higher at threefold acceleration than at twofold acceleration.

With increasing b-value, there is exponential loss of SNR. In a previous systematic study, the optimal b-value for DTI of the median nerve at 3 T was found to be in the range of 1,000–1,400 s/mm^2 [12]. In the present work, a b-value at the lower border of this range was used (1,000 s/mm^2) to ensure a high SNR. Given the short T2 relaxation time of surrounding skeletal muscle tissue, only little diffusion signal is left in muscles at this b-value level [36], which facilitates the depiction of the median nerve on the parametrical maps. We further optimized the SNR of the DTI sequence by partial Fourier sampling (5/8), as the thereby-achieved TE shortening increased the SNR [37]. As a compromise between SNR and spatial resolution, a moderate in-plane resolution and slice thickness were used. By lowering the spatial resolution, the SNR could be increased, but quantitative measurements and tractography would be impaired due to partial-volume effects. Other potential techniques that improve the SNR, such as multiple signal averages or additional gradient field directions, are limited by the cost of a longer acquisition time and thus the higher likelihood of motion artefacts.

Based on the results of the present work we advocate the use of twofold slice acceleration for DTI of the median nerve to halve the acquisition time while maintaining the image quality and SNR sufficient for parameter measurements and tractography. Although associated with comparable functional DTI metrics, the use of threefold slice acceleration for tractography of the median nerve is not supported by our results due to the lower SNR.

Our study has some limitations. First, a relatively small number of subjects was imaged. Because of the high reliability and low variability of the results, however, additional subjects would most likely not have changed them. Second, no patients were included in this initial feasibility study. Last, a bias was introduced as most study subjects were young individuals and it is known that DTI of the median nerve is age-dependent in terms of the diffusion metrics.

In conclusion, future DTI studies on peripheral nerves may strongly profit from twofold slice acceleration. The slightly decreased SNR is more than compensated for by the increase in SNR per time unit and the thereby-reduced likelihood of motion artefacts. It has still to be proven whether this technique yields comparable results in case of pathologies such as carpal tunnel syndrome, where DTI of the peripheral nerves currently has its main potential for clinical application [13, 18, 19].

Acknowledgments The authors kindly thank Heiko Meyer and Thomas Beck (both Siemens Healthcare, Erlangen, Germany) for providing them with the software for simultaneous multi-slice acquisition. The scientific guarantor of this publication is Roman Guggenberger, MD. Gustav Andreisek, MD, MBA, and Val M. Runge, MD, declare relationships with Siemens Healthcare, Erlangen, Germany. Himanshu Bhat, PhD is an employee of Siemens Medical Solutions USA Inc, Charlestown, MA, United States. These companies had no influence on the present study. The authors state that this work has not received any funding. No complex statistical methods were necessary for this paper. Institutional Review Board approval was obtained. Written informed consent was obtained from all subjects in this study. Methodology: prospective, experimental, performed at one institution.

References

1. Basser PJ, Mattiello J, LeBihan D (1994) MR diffusion tensor spectroscopy and imaging. Biophys J 66:259–267
2. Basser PJ, Jones DK (2002) Diffusion-tensor MRI: theory, experimental design and data analysis - a technical review. NMR Biomed 15:456–467
3. Mattiello J, Basser PJ, Le Bihan D (1997) The b matrix in diffusion tensor echo-planar imaging. Magn Reson Med 37:292–300
4. Basser PJ, Pajevic S, Pierpaoli C, Duda J, Aldroubi A (2000) In vivo fiber tractography using DT-MRI data. Magn Reson Med 44:625–632
5. Bammer R, Acar B, Moseley ME (2003) In vivo MR tractography using diffusion imaging. Eur J Radiol 45:223–234
6. Baumer P, Kele H, Kretschmer T et al (2014) Thoracic outlet syndrome in 3T MR neurography-fibrous bands causing discernible lesions of the lower brachial plexus. Eur Radiol 24:756–761
7. Schwarz D, Weiler M, Pham M, Heiland S, Bendszus M, Baumer P (2015) Diagnostic signs of motor neuropathy in MR neurography: nerve lesions and muscle denervation. Eur Radiol 25:1497–1503
8. Kasper JM, Wadhwa V, Scott KM, Rozen S, Xi Y, Chhabra A (2015) SHINKEI–a novel 3D isotropic MR neurography technique: technical advantages over 3DIRTSE-based imaging. Eur Radiol 25:1672–1677
9. Jengojan S, Kovar F, Breitenseher J, Weber M, Prayer D, Kasprian G (2015) Acute radial nerve entrapment at the spiral groove: detection by DTI-based neurography. Eur Radiol 25:1678–1683
10. Andreisek G, White LM, Kassner A, Sussman MS (2010) Evaluation of diffusion tensor imaging and fiber tractography of the median nerve: preliminary results on intrasubject variability and precision of measurements. AJR Am J Roentgenol 194:W65–W72

11. Andreisek G, White LM, Kassner A, Tomlinson G, Sussman MS (2009) Diffusion tensor imaging and fiber tractography of the median nerve at 1.5T: optimization of b value. Skelet Radiol 38:51–59
12. Guggenberger R, Eppenberger P, Markovic D et al (2012) MR neurography of the median nerve at 3.0T: optimization of diffusion tensor imaging and fiber tractography. Eur J Radiol 81:e775–e782
13. Guggenberger R, Markovic D, Eppenberger P et al (2012) Assessment of median nerve with MR neurography by using diffusion-tensor imaging: normative and pathologic diffusion values. Radiology 265:194–203
14. Guggenberger R, Nanz D, Bussmann L et al (2013) Diffusion tensor imaging of the median nerve at 3.0 T using different MR scanners: agreement of FA and ADC measurements. Eur J Radiol 82: e590–e596
15. Barcelo C, Faruch M, Lapegue F, Bayol MA, Sans N (2013) 3-T MRI with diffusion tensor imaging and tractography of the median nerve. Eur Radiol 23:3124–3130
16. Hiltunen J, Suortti T, Arvela S, Seppa M, Joensuu R, Hari R (2005) Diffusion tensor imaging and tractography of distal peripheral nerves at 3 T. Clin Neurophysiol 116:2315–2323
17. Khalil C, Hancart C, Le Thuc V, Chantelot C, Chechin D, Cotten A (2008) Diffusion tensor imaging and tractography of the median nerve in carpal tunnel syndrome: preliminary results. Eur Radiol 18:2283–2291
18. Lindberg PG, Feydy A, Le Viet D, Maier MA, Drape JL (2013) Diffusion tensor imaging of the median nerve in recurrent carpal tunnel syndrome - initial experience. Eur Radiol 23:3115–3123
19. Naraghi A, da Gama LL, Menezes R et al (2013) Diffusion tensor imaging of the median nerve before and after carpal tunnel release in patients with carpal tunnel syndrome: feasibility study. Skelet Radiol 42:1403–1412
20. Stein D, Neufeld A, Pasternak O et al (2009) Diffusion tensor imaging of the median nerve in healthy and carpal tunnel syndrome subjects. J Magn Reson Imaging 29:657–662
21. Pruessmann KP, Weiger M, Scheidegger MB, Boesiger P (1999) SENSE: sensitivity encoding for fast MRI. Magn Reson Med 42: 952–962
22. Feinberg DA, Crooks LE, Hoenninger JC et al (1986) Contiguous thin multisection MR imaging by two-dimensional Fourier transform techniques. Radiology 158:811–817
23. Larkman DJ, Hajnal JV, Herlihy AH, Coutts GA, Young IR, Ehnholm G (2001) Use of multicoil arrays for separation of signal from multiple slices simultaneously excited. J Magn Reson Imaging 13:313–317
24. Breuer FA, Blaimer M, Heidemann RM, Mueller MF, Griswold MA, Jakob PM (2005) Controlled aliasing in parallel imaging results in higher acceleration (CAIPIRINHA) for multi-slice imaging. Magn Reson Med 53:684–691
25. Setsompop K, Gagoski BA, Polimeni JR, Witzel T, Wedeen VJ, Wald LL (2012) Blipped-controlled aliasing in parallel imaging for simultaneous multislice echo planar imaging with reduced g-factor penalty. Magn Reson Med 67:1210–1224
26. Eichner C, Jafari-Khouzani K, Cauley S et al (2014) Slice accelerated gradient-echo spin-echo dynamic susceptibility contrast imaging with blipped CAIPI for increased slice coverage. Magn Reson Med 72:770–778
27. Chang WT, Setsompop K, Ahveninen J, Belliveau JW, Witzel T, Lin FH (2014) Improving the spatial resolution of magnetic resonance inverse imaging via the blipped-CAIPI acquisition scheme. NeuroImage 91:401–411
28. Roberts TP, Liu F, Kassner A, Mori S, Guha A (2005) Fiber density index correlates with reduced fractional anisotropy in white matter of patients with glioblastoma. AJNR Am J Neuroradiol 26:2183–2186
29. Price RR, Axel L, Morgan T et al (1990) Quality assurance methods and phantoms for magnetic resonance imaging: report of AAPM nuclear magnetic resonance Task Group No. 1. Med Phys 17:287–295
30. Landis JR, Koch GG (1977) The measurement of observer agreement for categorical data. Biometrics 33:159–174
31. Jones DK, Cercignani M (2010) Twenty-five pitfalls in the analysis of diffusion MRI data. NMR Biomed 23:803–820
32. Lau AZ, Tunnicliffe EM, Frost R, Koopmans PJ, Tyler DJ, Robson MD (2014) Accelerated human cardiac diffusion tensor imaging using simultaneous multislice imaging. Magn Reson Med. doi:10.1002/mrm.25200
33. Paley MN, Lee KJ, Wild JM, Griffiths PD, Whitby EH (2006) Simultaneous parallel inclined readout image technique. Magn Reson Imaging 24:557–562
34. Setsompop K, Cohen-Adad J, Gagoski BA et al (2012) Improving diffusion MRI using simultaneous multi-slice echo planar imaging. NeuroImage 63:569–580
35. Gambarota G, Mekle R, Mlynarik V, Krueger G (2009) NMR properties of human median nerve at 3 T: proton density, T1, T2, and magnetization transfer. J Magn Reson Imaging 29:982–986
36. Skorpil M, Engstrom M, Nordell A (2007) Diffusion-direction-dependent imaging: a novel MRI approach for peripheral nerve imaging. Magn Reson Imaging 25:406–411
37. Sinha S, Sinha U, Edgerton VR (2006) In vivo diffusion tensor imaging of the human calf muscle. J Magn Reson Imaging 24: 182–190